The EMBO Journal Vol.17 No.21 pp.6276–6288, 1998

Requirement of the mouse *I-mfa* gene for placental development and skeletal patterning

Norbert Kraut[1,5,6], Lauren Snider[1], C.-M.Amy Chen[3], Stephen J.Tapscott[1,4] and Mark Groudine[1,2]

[1]Fred Hutchinson Cancer Research Center, 1100 Fairview Ave N., A3-025, PO Box 19024, Seattle, WA 98109-1024, [2]Department of Radiation Oncology, University of Washington Medical School, Seattle, WA 98195, [3]Department of Genetics, Harvard Medical School, 200 Longwood Avenue, Boston, MA 02115 and [4]Department of Neurology, University of Washington Medical School, Seattle, WA 98195, USA

[5]Present address: Boehringer Ingelheim Pharma KG, Genomics Group, Birkendorfer Strasse 65, D-88397 Biberach an der Riss, Germany

[6]Corresponding author
e-mail: norbert.kraut@bc.boehringer-ingelheim.com

The bHLH-repressor protein I-mfa binds to MyoD family members, inhibits their activity, and blocks their nuclear import and binding to DNA. *In situ* hybridization analysis demonstrated that mouse *I-mfa* was highly expressed in extraembryonic lineages, in the sclerotome, and subsequently within mesenchymal precursors of the axial and appendicular skeleton, before chondrogenesis occurs. Targeted deletion of *I-mfa* in a C57Bl/6 background resulted in embryonic lethality around E10.5, associated with a placental defect and a markedly reduced number of trophoblast giant cells. Overexpression of *I-mfa* in rat trophoblast (Rcho-1) stem cells induced differentiation into trophoblast giant cells. I-mfa interacted with the bHLH protein Mash2, a negative regulator of trophoblast giant cell formation, and inhibited its transcriptional activity in cell culture. In contrast, I-mfa did not interfere with the activity of the bHLH protein Hand1, a positive regulator of giant cell differentiation. Interestingly, *I-mfa*-null embryos on a 129/Sv background had no placental defect, generally survived to adulthood, and exhibited delayed caudal neural tube closure and skeletal patterning defects that included fusions of ribs, vertebral bodies and abnormal formation of spinous processes. Our results indicate that I-mfa plays an important role in trophoblast and chondrogenic differentiation by negatively regulating a subset of lineage-restricted bHLH proteins.

Keywords: gene targeting/genetic background/I-mfa/skeletal patterning/trophoblast development

Introduction

Basic helix–loop–helix (bHLH) proteins regulate cell determination and differentiation during embryogenesis (for reviews see Jan and Jan, 1993; Weintraub, 1993). The *MyoD* subfamily of bHLH proteins (consisting of *MyoD*, *Myf5*, *myogenin* and *MRF4*) regulates both muscle cell determination and differentiation (reviewed by Weintraub, 1993; Rudnicki and Jaenisch, 1995), whereas members of the *NeuroD* and *Mash* (mammalian *achaete-scute* 1) subfamilies are involved in neuronal differentiation (reviewed by Lee, 1997), the *Scl* gene regulates hematopoiesis (Shivdasani *et al*., 1995), and the widely expressed *E2A* gene is required for B-cell formation (Bain *et al*., 1994; Zhuang *et al*., 1994). Additional bHLH factors are implicated as regulators of lineage commitment and differentiation: Hand2 (dHAND, Thing2, Hed) and Hand1 (eHAND, Thing1, Hxt) are involved in cardiac morphogenesis (Srivastava *et al*., 1997; Firulli *et al*., 1998; Riley *et al*., 1998); Mash2 and Hand1 play a role in trophoblast development (Guillemot *et al*., 1994; Cross *et al*., 1995; Firulli *et al*., 1998; Riley *et al*., 1998); Paraxis is required for somite formation (Burgess *et al*., 1996); and Scleraxis is implicated in regulating chondrogenesis (Cserjesi *et al*., 1995a; Liu *et al*., 1997). Commonly, more than one bHLH protein is expressed in a cell during development and it remains unknown whether the activity of co-expressed bHLH proteins is differentially regulated to achieve the coordinated expression of genes during development.

The first identified example of a negative regulator of bHLH proteins was the HLH protein Id, which lacks the basic domain responsible for DNA binding. Id family members can inhibit myogenesis by associating with the HLH domains of E-proteins and removing them from functional heterocomplexes with the myogenic bHLH proteins (Jen *et al*., 1992). The bHLH protein Mtwist also titrates E-proteins away from the myogenic bHLH proteins and prevents *trans*-activation of muscle target genes by the MEF2 family of myogenic regulatory factors (Spicer *et al*., 1996). The bHLH protein HES-1 can also inhibit the function of MyoD and represses myogenesis by inhibiting the MyoD/E2A complexes from binding to their target sequences (Sasai *et al*., 1992).

We recently identified a non-HLH inhibitor of the myogenic bHLH subfamily, I-mfa (Chen *et al*., 1996), based on the physical interaction between the C-terminus of I-mfa and the myogenic bHLH proteins. I-mfb and I-mfc are two additional proteins generated by alternative splicing that lack the I-mfa-specific C-terminus and do not interact with the myogenic bHLH proteins. I-mfa is localized predominantly in the cytoplasm and inhibits the function of myogenic bHLH proteins by at least two mechanisms: (i) I-mfa prevents nuclear localization of myogenic bHLH proteins by masking their nuclear localization signal; and (ii) when translocated to the nucleus, I-mfa also prevents DNA binding of myogenic bHLH proteins. I-mfa appears to target a subset of bHLH proteins, since it fails to inhibit nuclear translocation, DNA binding or transcriptional activity of E-proteins.

In this study, we show that *I-mfa* exhibits a complex

pattern of expression during mouse embryogenesis. High levels of expression were detected in extraembryonic tissues, as well as in the sclerotome and its derivatives, suggesting a role for I-mfa in multiple developmental processes. *I-mfa*-null embryos on a 129/Sv background were viable and showed skeletal patterning defects and delayed caudal neural tube closure. In contrast, *I-mfa* mutants on a C57Bl/6 background died during mid-gestation, associated with defects in trophoblast giant cell formation. Overexpression of *I-mfa* promoted differentiation of trophoblast giant cells and inhibited the activity of Mash2, a bHLH protein that blocks trophoblast giant cell differentiation, but did not inhibit the activity of Hand1, a bHLH protein that promotes giant cell differentiation. Our results indicate that I-mfa plays an important role in trophoblast and chondrogenic differentiation by negatively regulating a subset of lineage-restricted bHLH proteins.

Results

Targeted disruption of the mouse I-mfa gene

We generated two different *I-mf* mutations. The first mutation selectively replaced the entire domain of the *I-mfa*-specific exon V (codons 162–246 of *I-mfa*) that is required for direct protein–protein interaction with MyoD family members and for repression of myogenesis (Chen *et al*., 1996) with a neomycin selection cassette (Figure 1A). A second mutation deleted the coding sequence of all three *I-mf* isoforms (*I-mfa*, *I-mfb*, *I-mfc*). Both mutations had the same phenotype, indicating that the two additional isoforms, *I-mfb* and *I-mfc*, do not play essential roles during embryonic development. Data presented will be restricted to the specific deletion of the *I-mf* exon V, the *I-mfa*-specific exon.

Mice heterozygous for the *I-mfa* mutant allele were intercrossed to generate homozygous offspring. Southern blot and PCR analyses (Figure 1B and C) revealed that homozygous mice were present on a C57Bl/6×129/Sv hybrid background (Table I), while both Northern blot and RT–PCR analyses (Figure 1D and E) demonstrated that homozygous mutant embryos lack *I-mfa* mRNA, whereas *I-mfb* and *I-mfc* were expressed at normal levels. Interestingly, the phenotype and viability of mutant embryos was strain-dependent, showing a slightly reduced incidence of P7 offspring in the 129/Sv background and no P7 offspring in the C57Bl/6 background (Table I).

Skeletal patterning defects of I-mfa homozygous mutant embryos in a 129/Sv genetic background

At embryonic day 11.5 (E11.5), *I-mfa* was highly expressed in the chondrogenic center of the limb buds, in the sclerotome and rib primordia (Figure 2A). In addition, high-level expression was present in precursors of intervertebral discs and in developing vertebrae throughout the embryo (data not shown). Skeletal preparations from *I-mfa*–/– neonates ($n = 4$), E17.5 embryos ($n = 14$), and E13.5 embryos ($n = 9$) in a 129/Sv genetic background showed vertebral and rib defects in 90% of the mutant embryos, whereas the craniofacial and appendicular skeleton, including digit patterning, was normal. The rib defects consisted of fusions and bifurcations in the distal regions of the ribs on both sides of the sternum, truncated ribs

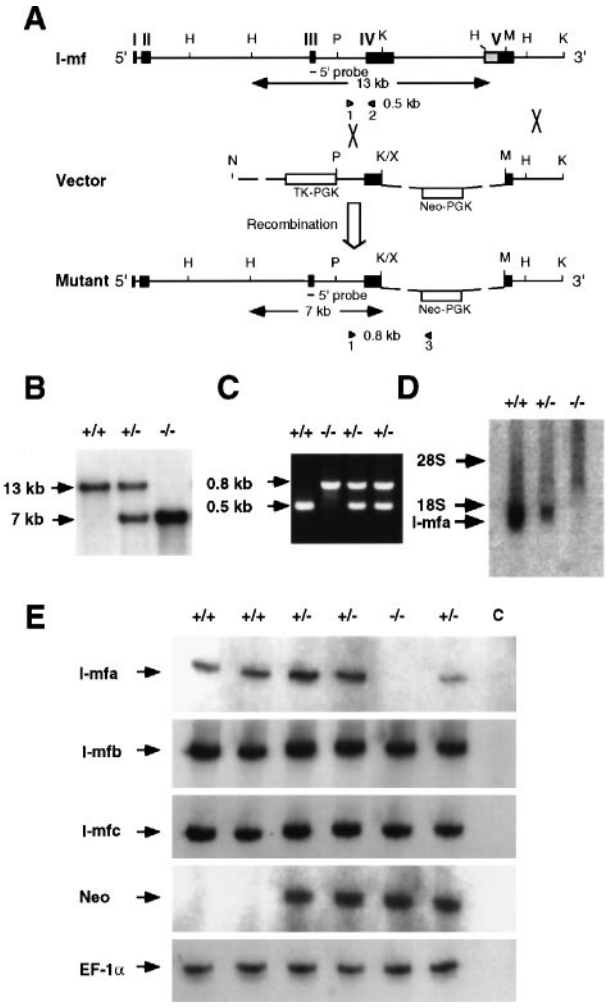

Fig. 1. Disruption of the *I-mf* gene by targeted recombination to generate *I-mfa* mutants. (**A**) Maps of the wild-type *I-mf* locus, the targeting vector and the mutant *I-mf* allele. Relative positions of the five *I-mf* exons (I, II, III, IV, V) are indicated by black boxes, the domain within exon 5 responsible for interaction with myogenic bHLH factors is indicated by a shaded box. The map of the targeting vector shows the replacement of the interactional domain in exon 5 and part of exon 4 (encoding the 3′UTR of *I-mfb*) by the *neomycin* resistance gene driven by the *PGK* enhancer (*PGKneo*) in reverse orientation, and the location of the flanking *HSV thymidine kinase* gene driven by *PGK* (*PGK-TK*) in reverse orientation. Open arrowheads denote the sites within the wild-type and the disrupted *I-mf* alleles from which PCR primers are derived; lines at the bottom indicate expected sizes for *Hin*dIII–*Xba*I-generated fragments detected with a 5′-flanking genomic probe from wild-type and disrupted *I-mf* alleles. H, *Hin*dIII; K, *Kpn*I; M, *Mlu*I; P, *Pst*I; X, *Xba*I. (**B**) Southern blot analysis of DNA from individual embryos (the progeny of a heterozygous mating). Sizes of the wild-type and targeted alleles are indicated by the 13 and 7 kb hybridizing bands, respectively. (**C**) PCR analysis of yolk sac DNA from individual embryos (the progeny of another heterozygous intercross), using primers 1, 2 and 3. Amplification of wild-type and mutant alleles by PCR yields products of 0.5 and 0.8 kb, respectively. (**D**) Detection of *I-mf* mRNA expression by Northern blot analysis in E14.5 embryos, using as a probe a cDNA fragment present in *I-mfa*, *I-mfb* and *I-mfc*. The *I-mfa* message is absent in I-mf mutant embryos. (**E**) Analysis of *I-mf* mRNA by semi-quantitative RT–PCR using RNA from E14.5 embryos. *I-mf*-null embryos have no detectable *I-mfa* transcript. No significant difference in *I-mfb* and *I-mfc* levels in the mutant versus wild-type embryos can be detected by this method. *EF-1*α expression was used as a control. The control (C) lanes are reactions containing cDNA from heterozygous embryos but lacking reverse transcriptase.

Table I. Genotype of offspring from *I-mfa* heterozygous parents

Age (days post-coitum)	Genotype of live and resorbing embryos[a]			Total embryos or mice
	+/+	+/–	–/–	
	129/Sv×C57Bl/6 (hybrid background)			
9.5+10.5	12 (21.4%)	27 (48.2%)	17 (30.3%; 2 dead)	56
11.5	13 (27.1%)	26 (54.1%)	9 (18.7%; 4 dead)	48
12.5	8 (25.0%)	19 (59.4%)	5 (15.6%; 2 dead)	32
13.5	10 (23.2%)	29 (67.4%)	4 (9.3%)	43
16.5+17.5	16 (25.0%)	42 (65.6%)	6 (9.4%)	64
P 7[b]	69 (31.5%)	133 (60.7%)	17 (7.8%)	219
	129/Sv background			
17.5+18.5	25 (26.6%)	45 (47.9%)	24 (25.6%)	94
P 7[b]	59 (32.6%)	91 (50.3%)	31 (17.1%)	181
	C57Bl/6 (third backcross generation)			
7.5	21 (26.9%)	37 (47.4%)	20 (25.6%)	78
8.5	27 (26.5%)	48 (47.1%)	27 (26.5%)	102
9.5	43 (22.6%)	98 (51.6%)	49 (25.8%; 1 dead)	190
10.5	14 (25.4%)	27 (49.1%)	14 (25.4%; 2 dead)	55
11.5	10 (24.4%)	22 (53.7%)	9 (22.0%; 8 dead)	41
17.5+18.5	15 (36.6%)	25 (60.1%)	1 (2.4%)	41
P 7[b]	67 (33.7%)	128 (64.3%)	4 (2.0%)	199
	C57Bl/6 (fifth backcross generation)			
P 7[b]	28 (35.0%)	52 (65.0%)	0 (0.0%)	80

[a]+/+, +/– and –/– refer to embryos wild-type, heterozygous and homozygous mutants for *I-mfa*.
[b]Postnatal day 7.

that fail to attach to the sternum and, in a few instances, the loss of one or more ribs (Figure 2B). Rib anomalies were apparent in E13.5 homozygous mutant embryos (Figure 2C), a stage at which cartilaginous rib primordia have formed but ossification has not begun, indicating that the mutation affected the outgrowth of the cartilaginous rib primordia.

Analysis of newborn homozygous *I-mfa* mutants showed that in addition to the rib defects, spinous processes failed to fuse medially in the lumbar and sacral region, resulting in a mild form of spina bifida. Instead, spinous processes were often observed to fuse in a cranial to caudal direction (Figure 2D and E). Moreover, skeletal preparations of E17.5 or newborn mutants showed that vertebral bodies can fuse laterally in the tail region (Figure 2H), giving rise to kinky and/or curly tails. Tail defects due to vertebral body fusions are often caused by a delayed neural tube closure (reviewed by Copp, 1994). In the mouse, the neural tube initiates closure at E8.5, beginning at the cervical/hindbrain boundary (Morriss-Kay *et al*., 1994) and later at two additional positions. Closure then spreads along the neural folds in the rostral and caudal directions. By E9.5, closure is normally complete. Sections of E11.5 *I-mfa* mutant embryos revealed a delay in the closure of the cranial neural tube, as shown with the dorsal neural tube marker *Pax-3* (Figure 2F and G). The delay in caudal neural tube closure starts in the lower lumbar/upper sacral region, similar to previously described mutants with this defect (reviewed in Copp, 1994), and therefore is a likely explanation for the vertebral body fusions in the tail regions and for the failure of spinous processes to fuse medially.

Approximately 75% of the *I-mfa* mutant mice with these types of skeletal defects showed a reduction in size and weight (on average 20% reduction), but could survive past weaning and were fertile. After more than 12 months of observation, no shortening of their lifespan has been noticed. However, the most severely affected mutants (~25% of mutants) with multiple rib fusions and in which several ribs failed to attach to the sternum, died shortly after birth. Their death was most likely due to respiratory distress associated with these rib defects (see also Braun *et al*., 1992; Yoon *et al*., 1997 and references therein). No additional defects, in particular no gross defects in muscle formation, were noticed (data not shown).

Molecular analysis of I-mfa null mutants on a 129/Sv genetic background

To investigate the early molecular events in cartilage formation, *in situ* hybridization to sclerotome-expressed genes was performed on mutant embryos between E11.5 and E12.5. *Pax-1* encodes a paired domain/homeodomain transcription factor. In the somite, its expression starts before E9.0 and is restricted to the medioventral region of the sclerotome (Deutsch *et al*., 1988; Wallin *et al*., 1994). In E11.5 *I-mfa* mutant embryos, *Pax-1* expression was not altered in the sclerotome (Figure 3A and B), and RNA analysis by Northern blotting showed a normal level of expression (Figure 3G).

Scleraxis encodes a bHLH protein expressed between E9.5 and E10.5 in the lateral and ventromedial sclerotome, and in the mesenchymal cells in the body wall and limb buds. Subsequently, *Scleraxis* RNA becomes restricted to the chondroblast precursors of the axial and appendicular skeleton, as well as the cranial mesenchyme prior to chondrogenic differentiation (Cserjesi *et al*., 1995a).

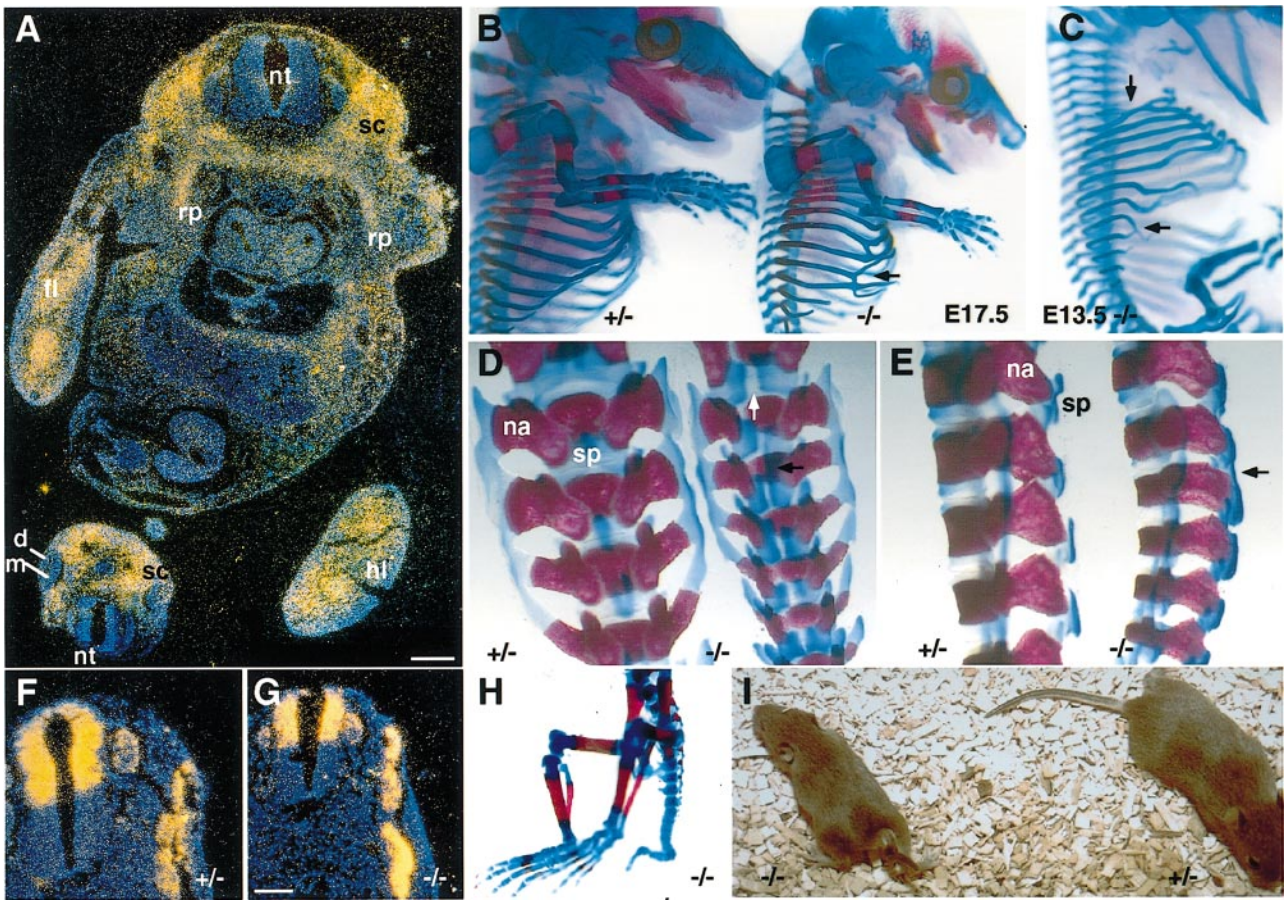

Fig. 2. Skeletal defects in *I-mfa* mutant mice on a 129/Sv background. (**A**) Expression of *I-mfa* within mesenchymal precursors of the axial and appendicular skeleton. d, dermatome; fl, forelimb; hl, hindlimb; m, myotome; nt, neural tube; rp, rib progenitors; sc, sclerotome. Scale bar = 390 μm. (**B**) Homozygous mutant (right) littermates at E17.5 show rib fusions and bifurcations (indicated by arrows). Onset of ossification (red staining) appears normally in mutant embryos. A heterozygous control littermate is shown on the left. (**C**) Homozygous mutant embryo at E13.5. Rib abnormalities were already present at E13.5 (arrow). To better view the rib cage, forelimbs were removed. (**D** and **E**) Abnormal fusions of spinous processes in *I-mfa* newborn mutants. Note that spinous processes (blue staining) in the mutant (right) fail to fuse medially (white arrow). In contrast, spinous processes can fuse cranial–caudally (black arrow). (D) Dorsal view; (E) lateral view. na, neural arch; sp spinous process. (**F** and **G**) Delay in closure of the dorsal neural tube in the caudal (immature) region of E11.5 embryos. (F) *Pax-3* expression in heterozygous *I-mfa* embryos; (G) *Pax-3* expression in homozygous mutant *I-mfa* embryos. Scale bar = 130 μm. (**H**) Tail of homozygous *I-mfa* mutant at E17.5, showing fusions between vertebral bodies in the tail region. (**I**) External appearance of *I-mfa* mutant (left) compared with a wild-type littermate (right) at 2 weeks of age.

Therefore, *Pax-1* and *Scleraxis* show distinct temporal expression patterns and demarcate different regions of the sclerotome, both of which express I-mfa. *Scleraxis* expression was reduced significantly in the sclerotome and in chondroblast precursors of the axial and appendicular skeleton in E11.5 *I-mfa* mutants (Figure 3C–F and H; also data not shown). These embryos exhibited a normal number of somites, and limb formation occurred at the appropriate time, indicating that the reduced *Scleraxis* expression was not due to a general delay of embryonic development. Furthermore, mutant embryos with only a small size reduction still showed a marked reduction in *Scleraxis* expression (not shown). Moreover, the expression of *Pax-9* (Neubüser *et al.*, 1995) in the lateral and ventromedial part of the sclerotome was reduced in *I-mfa* mutants (data not shown). Taken together, this analysis suggests that the medioventral region of the sclerotome develops normally, whereas the lateral and ventromedial sclerotome shows defective development, possibly resulting in the observed rib defects.

Mice lacking I-mfa on a C57Bl/6 genetic background die around E10.5 of gestation associated with a placental defect

As shown in Table I, on a hybrid C57Bl/6×129/Sv background, about two-thirds of the *I-mfa* mutants died around E10.5. Backcrosses into the C57Bl/6 genetic background led to a progressive decrease in the number of surviving *I-mfa* mutant embryos (4/199 mutant survivors on the third backcross generation and 0/80 mutant survivors on the fifth backcross generation). Almost all *I-mfa* mutant embryos of the third backcross generation died around E10.5. The first morphological abnormalities of *I-mfa* mutant embryos were recognized at E9.5, when they showed developmental retardation. Most of the mutant embryos had not yet completed 'turning', a process normally initiated at E8.5 that reverses the orientation of the germ layers. In addition, more than half of the embryos displayed an undulated neural tube (data not shown). Early cardiac morphogenesis appeared normal, including heart looping and the cardiac expression of *Hand1* and *Hand2*

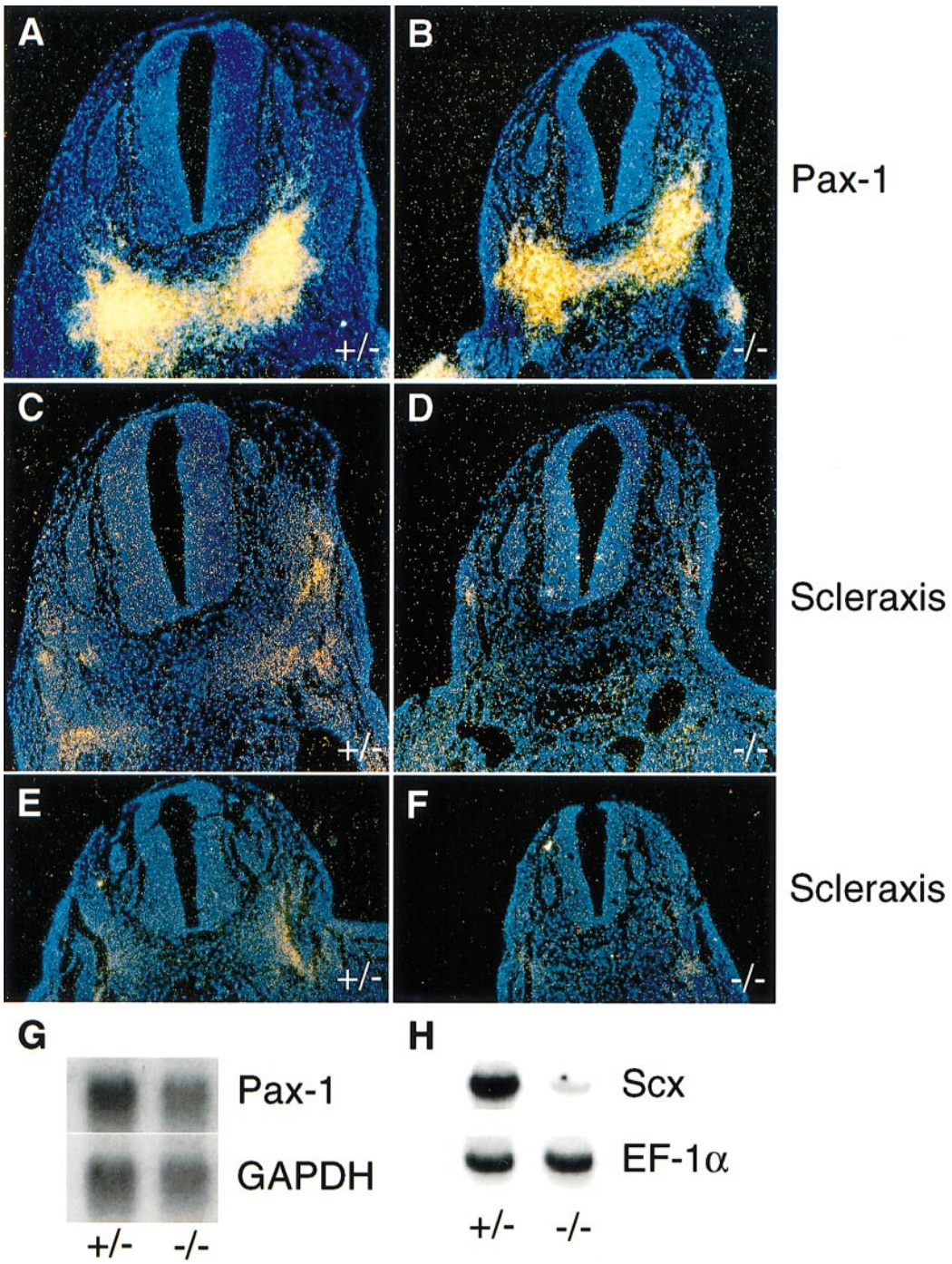

Fig. 3. Molecular analysis of sclerotomal markers in I-mfa heterozygous (A, C, E) and mutant (B, D, F) embryos at E11.5 by *in situ* hybridization (A–F), Northern blot analysis (G) and RT–PCR analysis (H). (**A** and **B**) *Pax-1* expression in the medioventral region of the sclerotome in heterozygous *I-mfa* embryos at the forelimb level (A) is unaltered in homozygous *I-mfa* mutant embryos (B). (**C** and **E**) *Scleraxis* expression in the sclerotome of E11.5 *I-mfa* heterozygous embryos. *Scleraxis* is normally expressed in the lateral and ventromedial sclerotome. (**D** and **F**) In *I-mfa*–/– embryos, *Scleraxis* expression is reduced. (C, D) Sections at forelimb level; (E) section at hindlimb level; (F) section slightly cranial to hindlimb level. Scale bars: (A–E) = 130 μm. (**G**) Northern blot analysis of embryos showed normal *Pax-1* levels in *I-mfa* mutants when compared with *GAPDH* levels. (**H**) RT–PCR analysis of *Scleraxis* mRNA levels in *I-mfa*-null embryos. *I-mfa* heterozygous and null embryos were collected at E11.5 and RNA was prepared. *EF-1*α used as a control shows identical mRNA levels, whereas *Scleraxis* mRNA levels are reduced.

(data not shown). To determine the expression pattern of *I-mfa* in the embryos before lethality, we analyzed its expression by *in situ* hybridization.

At E7.5, *I-mfa* was detected in extraembryonic tissues (Figure 4A and B), including the ectoplacental cone, trophoblast giant cells and parietal endoderm, the chorion and the allantois, but not in the maternal decidua or amnion. Only a low level of *I-mfa* expression was detected in the embryo proper in the intraembryonic mesoderm of the future headfold region (Figure 4B). At E10.5, *I-mfa* was detected in trophoblast giant cells, spongiotrophoblasts and labyrinthine trophoblasts (Figure 4E), whereas expression was not observed in *I-mfa* mutants (Figure 4F). In addition to *I-mfa* expression in the extraembryonic tissues, we found high expression levels in the cephalic mesenchyme, but absence in the neural folds of the forebrain

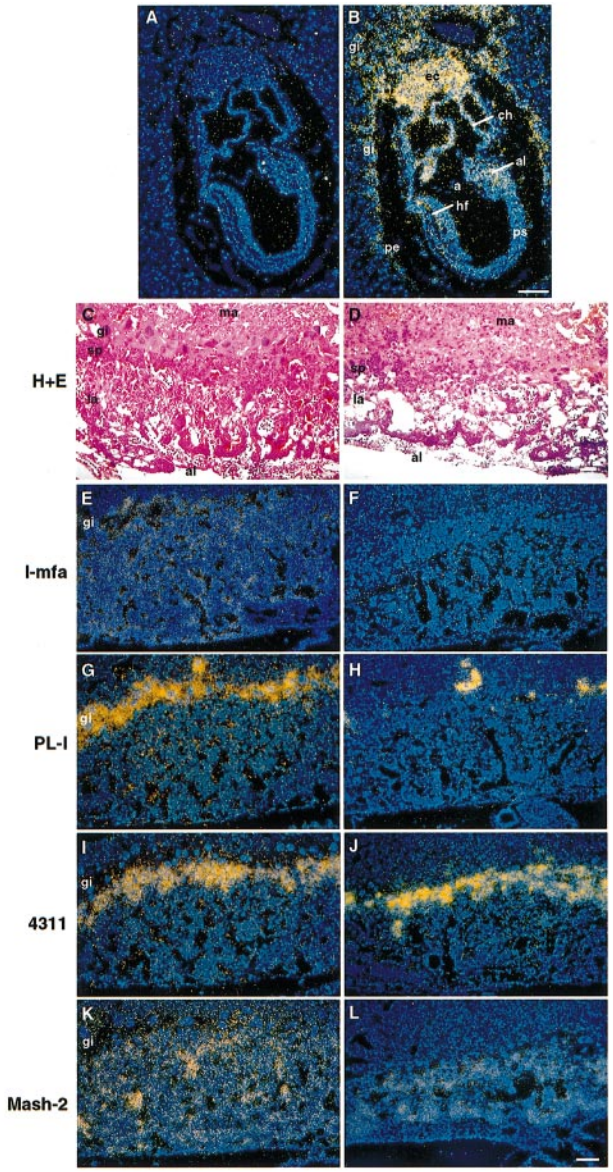

Fig. 4. Placental defect in *I-mfa* mutants on a C57Bl/6 background. (**A**) Hybridization to sagittal sections of an E7.5 mouse embryo with an *I-mfa* sense probe results in no specific hybridization. (**B**) Hybridization of an adjacent section with an *I-mfa* antisense probe. a, amnion; al, allantois; ch, chorion; ec, ectoplacental cone; gi, trophoblast giant cells; hf, future head fold; pe, parietal endoderm; ps, primitive streak. Scale bars (A,B) = 130 μm. (**C** and **D**) E10.5 placentas from normal (C) and I-mfa mutant (D) littermates. The trophoblast giant cells (gi) are reduced in number, and the labyrinthine trophoblast (la) appears slightly less compact, whereas the spongiotrophoblasts (sp) appear normal in mutant compared with normal placentas. Allantoic fusion (al) has occurred normally in the mutant; maternal tissue (ma) is as indicated. Sections were stained with hematoxylin and eosin (H+E). (E–L) Expression of molecular markers in E10.5 placentas from wild-type (E, G, I, K) and mutant (F, H, J, L) littermates analyzed by *in situ* hybridization of near-adjacent sections. (**E**) *I-mfa* transcripts are present in trophoblast giant cells, spongiotrophoblasts and labyrinthine trophoblasts. (**F**) *I-mfa* transcripts are absent in mutant placentas. The number of *PL-I*-expressing trophoblast giant cells is reduced markedly in *I-mfa* mutants (**H**) compared with wild-type (**G**). (**I** and **J**) Expression of *4311* mRNA which marks spongiotrophoblast cells in the placenta is normal in *I-mfa* mutants. (**K** and **L**) *Mash2* transcripts are present at normal levels in spongiotrophoblasts and labyrinthine trophoblasts in the placenta; (L) shows a mutant placenta with a more affected spongiotrophoblast layer. gi, giant trophoblast cell layer. Scale bars (C–L) = 130 μm.

and hindbrain. Expression was also found in the branchial arches, neural crest cells, the developing heart and the surrounding pericardium. Furthermore, *I-mfa* was expressed at low levels in the neural epithelium in the primitive streak region, in the presomitic mesoderm, in the hindgut and in the epidermis. No significant *I-mfa* expression was detected in the yolk sac, the dorsal aorta and the neural tube (data not shown).

I-mfa mutants showed a normal development of the chorion, the allantois and the yolk sac, including its vascularization (data not shown). Histologic analysis of the plancentas revealed a decreased number of trophoblast giant cells (Figure 4C and D), whereas the spongiotrophoblast layer appeared normal. *In situ* hybridization using a probe to detect transcripts of *(PL)-I*, which are restricted to trophoblast giant cells (Carney *et al*., 1993), revealed a strong reduction in the number of *PL-I*-positive cells in the placentas of *I-mfa* mutant embryos at E10.5. In addition, the few trophoblast giant cells detectable in *I-mfa* mutant placentas appeared to express higher levels of *PL-I* than those of normal embryos (Figure 4G and H). Since both trophoblast giant cells and spongiotrophoblasts are derived from diploid trophoblast progenitor cells in the ectoplacental cone, we investigated if the spongiotrophoblast layer was also altered. However, spongiotrophoblasts expressing the specific markers *4311* (Lescisin *et al*., 1988) and *Flt-1* (Guillemot *et al*., 1994) were found to be unaffected in *I-mfa* mutants at E10.5 (Figure 4I and J; also data not shown). The *Mash2* gene is expressed in spongiotrophoblasts, labyrinthine trophoblast cells and their precursors (Guillemot *et al*., 1994). At E10.5, there was a slight reduction in the number of *Mash2*-positive labyrinthine trophoblast cells in some mutant embryos, whereas spongiotrophoblasts expressing the *Mash2* gene were found to be unaffected (Figure 4K and L).

These results suggest that on the C57Bl/6 genetic background, I-mfa is necessary for the normal development of trophoblast giant cells, and that lethality around E10.5 most likely arises from the reduction in giant cell number, leading to placental failure. To determine whether the decreased trophoblast giant cell number was due to a low proliferation rate or to increased apoptosis, we examined 5-bromo-2′-deoxyuridine (BrdU) incorporation and TUNEL labeling (Gavrieli *et al*., 1992). No significant difference in the proliferative index and the intensity of staining of BrdU-positive cells was detected between wild-type and mutant embryos and extra-embryonic regions between E7.5 and E9.5 (data not shown). In *I-mfa* mutants, TUNEL assays showed a higher rate of apoptosis in secondary giant trophoblast cells as well as in their precursor cells located in the ectoplacental cone (Figure 5A and B). At E7.5, wild-type embryos had 0.4 ± 0.2 TUNEL-positive trophoblast cells per section, whereas mutant embryos had 3.5 ± 1.2 TUNEL-positive trophoblast cells. Moreover, TUNEL assays of E10.5 placentas showed that most of the remaining trophoblast giant cells in *I-mfa* mutants undergo apoptosis (Figure 5C and D). This result indicates that I-mfa is necessary for trophoblast giant cell survival in the C57Bl/6 background.

I-mfa promotes Rcho-1 trophoblast cell differentiation and inhibits Mash2 activity

Giant trophoblast cells arise from the diploid trophoblast cells in the ectoplacental cone, starting around E7.5 (Ilgren,

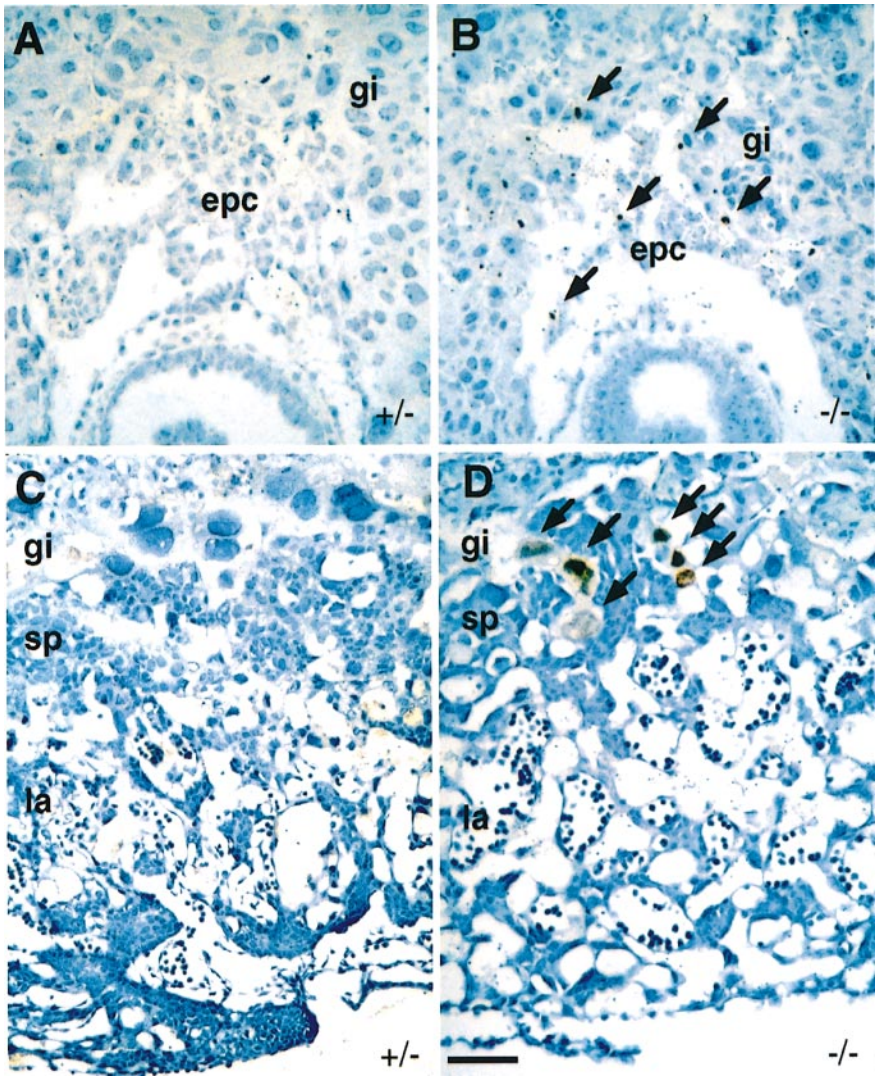

Fig. 5. Increased cell death observed in sections of *I-mfa* mutants. (**A**) E7.5 normal embryo subjected to the TUNEL reaction. (**B**) E7.5 *I-mfa* mutant embryo subjected to the TUNEL reaction. Sections showing diploid cells of the ectoplacental cone (epc) surrounded by differentiating secondary trophoblast giant cells (gi). (**C**) E10.5 normal placenta and (**D**) E10.5 *I-mfa* mutant placenta subjected to the TUNEL reaction. gi, trophoblast giant cells; sp, spongiotrophoblasts; la, labyrinthine trophoblast. Brown-stained nuclei indicate end incorporation in DNA and are marked by arrows. Sections were stained with Gill's hematoxylin #3. Scale bars (A–D) = 260 μm.

1983). Two bHLH proteins, Mash2 and Hand1, regulate giant trophoblast development. Mash2 inhibits giant cell formation and maintains proliferating trophoblasts (Guillemot *et al*., 1994; Cross *et al*., 1995). Mice with null mutations of *Mash2* have an increased number of trophoblast giant cells (Guillemot *et al*., 1994; Tanaka *et al*., 1997). In contrast, Hand1 promotes the differentiation of trophoblast cells into giant cells (Cross *et al*., 1995), and *Hand1*-null mutants show a significant giant-cell deficiency (Firulli *et al*., 1998; Riley *et al*., 1998). To investigate whether I-mfa could regulate this activity of Mash2 or Hand1, we used the Rcho-1 (rat choriocarcinoma) cell line that can differentiate into trypsin-resistant giant cells that express trophoblast giant cell markers (Faria and Soares, 1991; Cross *et al*., 1995). *I-mfa* mRNA levels increased during Rcho-1 differentiation (Figure 6A). *Hand1* and *PL-I* transcripts were strongly induced with differentiation (Figure 6A), whereas *Mash2* transcripts decreased (data not shown), consistent with previous findings (Faria and Soares, 1991; Cross *et al*., 1995).

Overexpression of *Mash2* reduced slightly, while *Hand1* increased significantly, the level of *PL-I* expression (Figure 6B), as well as the number of adherent cells (Figure 6C), was in agreement with similar findings by Cross *et al*. (1995). Similar to *Hand1* expression, overexpression of *I-mfa* increased *PL-I* expression (Figure 6B) and increased the number of adherent cells (Figure 6C). Moreover, stable overexpression of *I-mfa* in Rcho-1 stem cells resulted in a high percentage of morphologically differentiated giant cells, even under non-differentiation conditions (Figure 6D and E).

Expression analysis indicated that *I-mfa* was co-expressed with *Mash2* and *Hand1* in diploid trophoblast stem cells (Figure 4B; Guillemot *et al*., 1994; Cross *et al*., 1995; data not shown), suggesting that I-mfa might regulate trophoblast development by interacting with Mash2, Hand1 or other bHLH proteins in these cells.

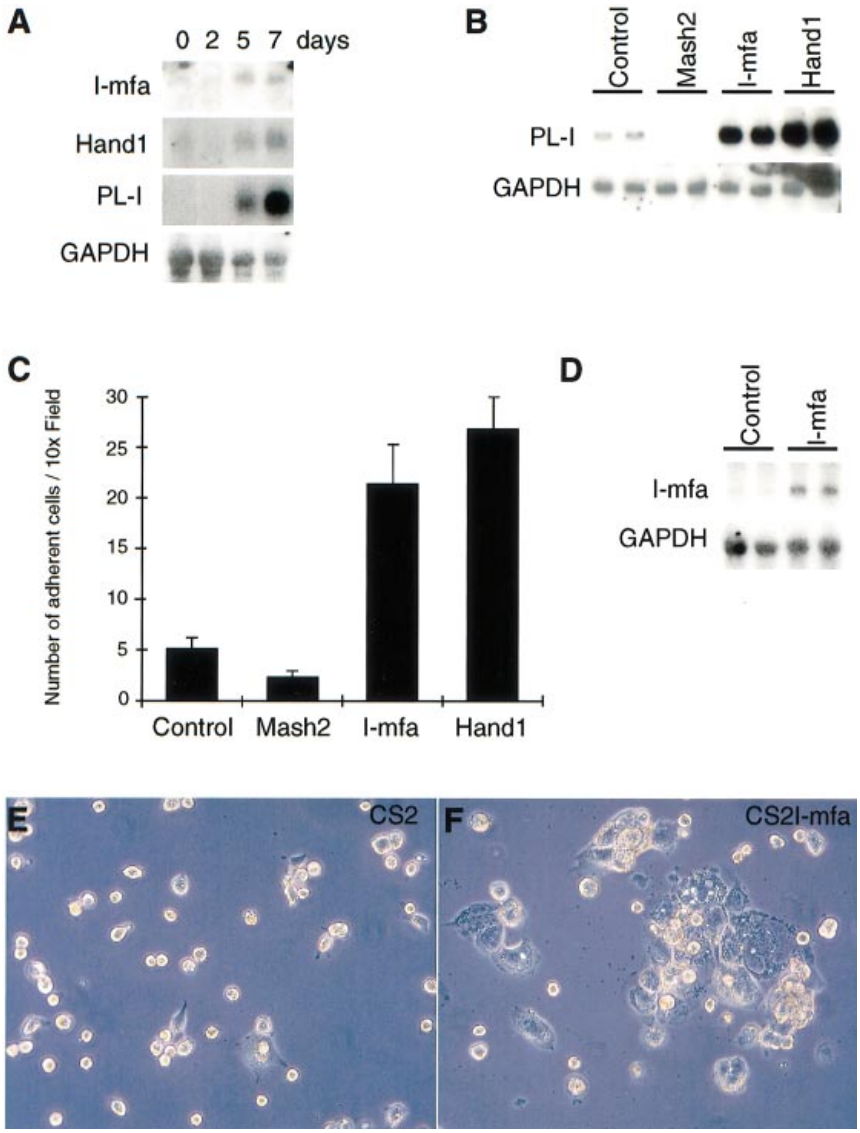

Fig. 6. I-mfa promotes Rcho-1 trophoblast giant cell differentiation. (**A**) Northern blot analysis of gene expression during trophoblast cell differentiation. Total RNA (10 μg) was harvested from stem cells grown in 20% FBS (day 0) or grown in 10% horse serum for 2, 5 or 7 days. RNAs were probed with cDNA probes for *I-mfa*, *Hand1*, *PL-I* and *GAPDH* (control). (B,C) Effect of transiently transfected Mash2, I-mfa, and Hand1 on Rcho-1 cell differentiation. Rcho-1 stem cells were transiently transfected with respective expression vectors and shifted to 10% horse serum for 3 days. (**B**) All cells were harvested after 3 days and subjected to Northern blot analysis (two independent experiments each), using *PL-I* and *GAPDH* (control) as probes. (**C**) Stem cells were removed by brief trypsinization and the adherent (differentiated) cells were counted (error bars indicate SD). (D–F) Stable overexpression of *I-mfa* promotes giant cell differentiation under non-inducing conditions. (**D**) Level of *I-mfa* expression determined by Northern blot analysis upon stable transfection of CS2I-mfa, compared with *I-mfa* expression in cells transfected with an empty CS2 vector. (**E**) Rcho-1 cells transfected with CS2 vector in 20% FBS maintain stem cell morphology. (**F**) Rcho-1 cells transfected with CS2I-mfa and maintained in 20% FBS differentiate at a high rate into trophoblast giant cells.

Yeast two-hybrid assays demonstrated that I-mfa interacted physically with both Mash2 and Hand1 (Figure 7A) with an affinity that was comparable with the interaction with myogenin (Figure 7A; see Chen *et al*., 1996). Interaction of I-mfa with Mash2 and Hand1 required the C-terminal region of the I-mfa isoform that is lacking in the I-mfb and I-mfc isoforms (data not shown). Therefore, the interactional domain in I-mfa with Mash2 and Hand1 is identical to the region required for its interaction with myogenic factors (see Chen *et al*., 1996). I-mfa failed to interact with E12, as shown previously (Chen *et al*., 1996). I-mfa also did not interact with Id1, a putative inhibitor of giant cell differentiation (Cross *et al*., 1995).

There are at least two potential mechanisms by which I-mfa might promote giant cell differentiation: (i) an inhibition of Mash2 activity; or (ii) the stimulation of Hand1 activity. We therefore examined the effect of I-mfa on Mash2- and Hand1-dependent transcriptional activity. In NIH 3T3 cells, I-mfa very efficiently inhibits Mash2 activity on a 4R-CAT reporter construct containing four multimerized E-boxes from the MCK enhancer (Figure 7B). The extent of repression of Mash2 activity by I-mfa was in the same range as its previously described repression of myogenin activity (Chen *et al*., 1996). In contrast, I-mfa had no significant effect on E12-dependent activation of this reporter construct. Since Hand1 did not activate the 4R-reporter construct in NIH 3T3 cells (data not shown), we used a reporter driven by the PL-I promoter

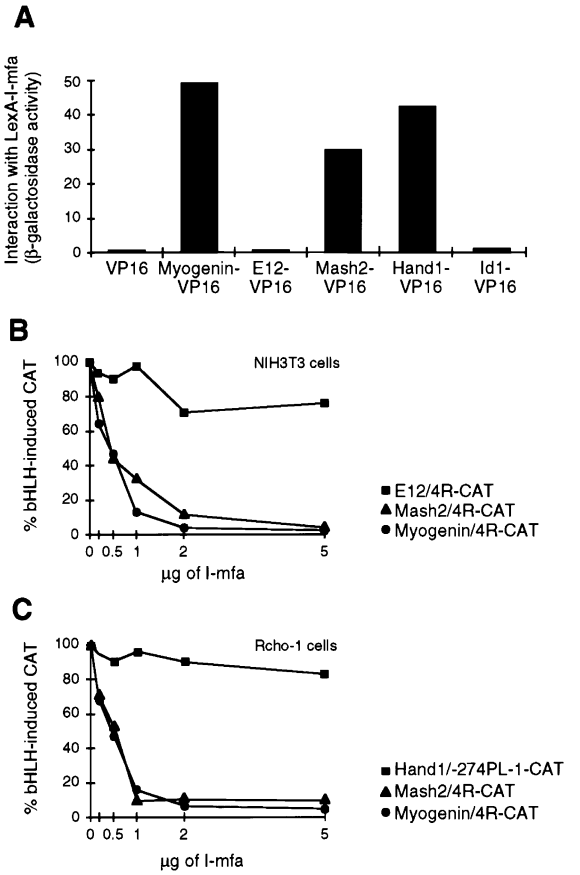

Fig. 7. Functional interaction of I-mfa with Mash2, but not Hand1. (**A**) A yeast two-hybrid interaction assay, using LexA-I-mfa and VP16 fusions with myogenin, E12, Mash2, Hand1 and Id1, revealed selective interaction of I-mfa with myogenin, Mash2 and Hand1. (**B**) NIH 3T3 cells were co-transfected with 2 µg expression plasmids encoding E12, Mash2 or myogenin, together with the p4R–CAT reporter gene (5 µg) and increasing amounts of CS2I-mfa (0–5 µg). (**C**) I-mfa (0–5 µg) and bHLH factors (2 µg) were co-transfected into Rcho-1 cells, using either p4R-CAT (for Mash2 and myogenin) or –274PL-I-CAT (for Hand1) as a reporter. Cells in (B) and (C) were assayed after three days for CAT activity. No reporter gene expression in (B) and (C) was detected in the control transfections (without bHLH expression construct) or with I-mfa alone. Similar results were obtained in three separate experiments. Duplicate determinations differed by <20%.

(Shida *et al*., 1993) that can be activated by Hand1 in proliferating Rcho-1 cells (Cross *et al*., 1995). We failed to see any significant effect of I-mfa on Hand1 activity (Figure 7C). As controls, I-mfa in Rcho-1 cells again strongly reduced the activity of Mash2 and myogenin on the responsive 4R-CAT reporter (Figure 7C). These results indicate that I-mfa may control giant cell differentiation by negatively regulating the activity of Mash2, a repressor of giant cell formation, and not by interfering with the activity of Hand1, a stimulator of giant cell differentiation.

Discussion

To understand the roles of *I-mfa* during development, we have studied its expression and the phenotypic consequences of an inactivating mutation. *In situ* hybridization showed expression in many tissues, most notably in extraembryonic lineages and the sclerotome. Targeted disruption demonstrated that the *I-mfa* gene is required for the proper formation of the skeleton, closure of the caudal neural tube and, dependent on genetic background, the generation of trophoblast giant cells. Our results reveal a good correlation between the sites of abundant *I-mfa* expression and the developmental defects observed in its absence, and suggest that I-mfa affects the activity of a subset of lineage-specific bHLH proteins.

Genetic background differences in I-mfa mutants

In our analysis of *I-mfa* mutant mice, we found that the placental defect of the null phenotype depends on whether the mutation is in the C57Bl/6 or 129/Sv genetic background, suggesting the existence of at least one modifier locus. Interestingly, a placental defect dependent upon genetic background has been described previously in *EGFR* mutant embryos (Sibilia and Wagner, 1995; Threadgill *et al*., 1995). We have excluded the possibility that *I-mfa* itself is expressed in a strain-dependent manner and preliminary results indicate that a single locus from the 129/SV background is sufficient to rescue the lethality (N.Kraut, unpublished results).

I-mfa is not required for formation of epithelial somites and their early patterning

We have shown that *I-mfa* is expressed at low levels in the presomitic mesoderm and in epithelial somites. Subsequently, *I-mfa* expression becomes restricted to the sclerotome and sclerotome-derived cells, whereas it is excluded from the myotome (Chen *et al*., 1996). Although not detailed in this manuscript, the initial formation of epithelial somites and their patterning into dermomyotome and sclerotome appeared to be normal in homozygous null mutants in both the C57Bl/6 and 129/Sv background, as judged by the expression of the somite markers *Mox1*, *paraxis*, *Myf5*, *myogenin* and *Pax-1* (N.Kraut, unpublished data). This result suggests that I-mfa does not restrict the spatial or temporal expression of MyoD family members during the early stages of somitogenesis. Alternatively, the absence of *I-mfa* may be compensated for *in vivo* by other myogenic repressors, for example *M-twist*, *Id1* and *Id3*, which show an overlapping expression pattern with *I-mfa* during somitogenesis (Wolf *et al*., 1991; Wang *et al*., 1992; Ellmeier and Weith, 1995; N.Kraut, unpublished results). These possibilities can be distinguished by generating compound mutants for these genes.

I-mfa regulates sclerotome development

I-mfa transcripts were expressed at high levels in the prevertebrae and in the rib primordia at E11.5 (Figure 2A), well before the onset of chondrogenesis between E12.5 and E14.0 (Rugh, 1990). *I-mfa*-null embryos showed several skeletal patterning defects, including fusions and bifurcations of ribs. Our experiments suggest that *I-mfa* mutant cells are able to differentiate into migrating and condensing medioventral sclerotome cells that express *Pax-1*. In contrast, we observed a marked reduction in the level of *Scleraxis*, a bHLH transcription factor implicated in regulating gene expression in chondrogenic lineages that is expressed in the lateral and ventromedial sclerotome and in chondrogenic migrating mesenchymal cells (Cserjesi *et al*., 1995a; Liu *et al*., 1997). This observation suggests that I-mfa has a role in modulating the differentiation of *Scleraxis*-expressing chondrogenic cells. The Scleraxis

protein heterodimerizes with E-proteins and activates transcription on a subset of E-boxes (Cserjesi *et al*., 1995a). We found that I-mfa can interact with Scleraxis in a yeast two-hybrid assay and counteracts Scleraxis activity on Scleraxis-dependent reporter constructs in transfection experiments (N.Kraut, unpublished results). These observations suggest that I-mfa might negatively modulate the activity of scleraxis during chondrogenesis and the skeletal phenotype could result from unregulated scleraxis activity, although I-mfa might also interact with other regulators of chondrogenesis.

It has been suggested that spina bifida and tail defects result from disturbed closure of the posterior neuropore (reviewed by Copp, 1994). Mechanisms underlying the delay of posterior neural tube closure are largely unknown. In some instances, this delay can result from a primary defect in the neuroepithelium, or from a defect in the notochord and hindgut endoderm causing ventral curvature of the neural tube region and inhibiting closure (Copp, 1994). *I-mfa* mutants exhibited a delayed neural tube closure, tail defects and an impaired closure of spinous processes. Therefore, the delay in neural tube closure is likely the cause for the formation of kinky tails, and may also be the cause for the failed closure of spinous processes. In contrast, fusions of spinous processes in a cranial–caudal manner may not be caused by the delay in neural tube closure, but more likely result from a defect in cartilage formation. Alternatively, spinous process fusions may result from defects in somite segmentation. Our marker analysis using early somite markers (*Paraxis*, *Mox1*, *Pax-9*), however, did not reveal any obvious early segmentation defects.

I-mfa is required for placental development

During mammalian development, the trophoblast is the first cell lineage to differentiate, giving rise to most of the extraembryonic tissues required for implantation (Cross *et al*., 1994). Later in the development, the chorioallantoic placenta contains three trophoblast-derived layers: the labyrinthine trophoblasts, spongiotrophoblasts and trophoblast giant cells (Cross *et al*., 1994). The observed growth retardation of the *I-mfa*-null embryos in the C57Bl/6 background and their subsequent death by E10.5 is consistent with a failure of placental function. A trophoblast defect can limit embryonic growth and development at E10–11, when circulation through the umbilical vessels is a primary source of nutrition for the embryo (Copp, 1995). *I-mfa* mutant embryos exhibited a dramatic reduction in the number of trophoblast giant cells, suggesting an important role of I-mfa in the differentiation of trophoblast stem cells. The issue of whether the lethality of *I-mfa*-null embryos at E10.5 in the C57Bl/6 background is exclusively placental and not embryonic can eventually be addressed by tetraploid rescue experiments (Nagy *et al*., 1990).

Control of trophoblast giant cell formation by the bHLH inhibitor I-mfa

Previous genetic studies have demonstrated that several bHLH proteins control the differentiation of secondary giant cells from the diploid trophoblast cells in the ectoplacental cone. Mash2 has been shown to play a cell autonomous role in maintaining the diploid trophoblast population by either supporting cell proliferation or inhibiting differentiation of these cells into giant cells (Guillemot *et al*., 1994; Tanaka *et al*., 1997), as suggested also by *in vitro* experiments with Rcho-1 cells (Cross *et al*., 1995). Hand1 is necessary to turn off Mash2 expression (Riley *et al*., 1998) and Hand1 mutants show a severe deficiency in trophoblast giant cells (Firulli *et al*., 1998; Riley *et al*., 1998). Thus, Hand1 could act either by promoting differentiation of ectoplacental cone cells into giant cells directly, or by negatively regulating *Mash2* expression, thereby allowing differentiation to occur. This differentiation switch is irreversible since giant cells enter an unusual cell cycle in which the cells remain postmitotic but undergo rounds of DNA replication (endoreduplication). Therefore, Mash2 and Hand1 potentially regulate the balance between maintenance of trophoblast cells with proliferative potential and terminal differentiation of trophoblast giant cells.

Our study of *I-mfa* mutants indicates that I-mfa is also required for the formation of trophoblast giant cells, since the number of giant cells is strongly reduced in *I-mfa* mutants in the C57Bl/6 background. Failure to normally execute terminal differentiation into trophoblast giant cells is the most likely cause for the observed cell death in the *I-mfa* mutant trophoblast lineage. Consistent with this, overexpressing *I-mfa* in Rcho-1 cells promotes giant cell differentiation. Interestingly, I-mfa can efficiently counteract Mash2 activity on a responsive reporter construct, while it fails to inhibit Hand1 activity. Since I-mfa and Mash2 interact in a yeast two-hybrid system and are co-expressed in giant cell precursors, we propose that I-mfa inhibits Mash2 activity by direct protein–protein interaction and that the phenotype of *I-mfa* mutants may be a result of unregulated Mash2. Similar to the inhibition of myogenic factors (Chen *et al*., 1996), I-mfa may inhibit Mash2 activity by preventing nuclear import and DNA binding. These questions can now be addressed using *I-mfa* mutant embryos. It will furthermore be interesting to cross the *I-mfa*-deficient mice with *Mash2* mutants, to determine if the early embryonic lethality of each single mutant can be rescued in a double mutant.

It has been speculated previously that the activities of different bHLH proteins in the same cell can be differentially regulated by varying the availability of an essential cofactor, such as an E-protein (Weintraub *et al*., 1991). Id proteins could play a role in regulating this balance, as they dimerize with widely expressed E-protein family members and limit their availability for interaction with other bHLH proteins. I-mfa represents a different strategy for differentially regulating the activities of co-expressed bHLH proteins. I-mfa inhibition of Mash2 activity, but not Hand1 activity, in trophoblast cells could represent a critical regulatory step, determining whether the cell will differentiate into a giant trophoblast cell or continue replicating as a trophoblast stem cell. We speculate that I-mfa plays a similar role in other lineages that express multiple bHLH proteins. For this model to be attractive, however, we must further speculate that the activity of I-mfa is regulated and responsive to environmental signaling. While we do not know whether the activity of I-mfa can be regulated, one possible mechanism would be that I-mfb or I-mfc can inhibit the activity of I-mfa. If this were the case, it would be consistent with the finding

that the elimination of all three transcripts has the same phenotype as eliminating only the I-mfa transcript.

Materials and methods

Generation of I-mfa mutant mice

Genomic phage λ clones encompassing the *I-mf* locus (MGD nomenclature: *Mdfi*; Kraut, 1997) were isolated by screening a 129/Sv genomic library (a kind gift of P.Soriano, FHCRC). Mapping and partial sequencing of the genomic locus revealed the exon–intron structure and the alternative splicing pattern of the *I-mf* gene (N.Kraut, C.-M.Amy Chen and M.Groudine, in preparation). The targeting vector consists of 2.7 kb of 5′- and 3.2 kb of 3′-genomic homology and a 4.8-kb deletion is introduced. The 5′ arm was generated by assembly of a 2.1-kb *Bam*HI fragment (Intron III), a 0.6-kb *Bam*HI–*Kpn*I fragment (Intron III to Exon IV just upstream of the stop codon of *I-mfb*), and a *Kpn*I–*Xba*I linker (5′-CCACGGGGTGGGAAAAGAGTTCTAACTCCAATAAGATCTTCTAGAGGTAC-3′) that reconstitutes the stop codon of *I-mfb* and contains an *Xba*I site at its 3′ end which allows cloning of the entire *Bam*HI–*Xba*I fragment into the *Bam*HI–*Xba*I site of pPNT (Tybulewicz *et al*., 1991). The 3′ arm was generated by ligation of a blunt-ended *Mlu*I–*Kpn*I fragment into the blunted *Xho*I site of pPNT. The targeting vector (25 μg) was linearized with *Not*I and electroporated into 1×10^7 AK-7 ES-cells (a gift from A.Imamoto and P.Soriano; BTX Transfector 300; 250 V, 500 μF). The cells were subsequently cultured in the presence of G418 (150 μg/ml; added 1 day later) and 2 μg/ml gancyclovir (added 3 days later), essentially as described (Hogan *et al*., 1994). Homologous recombinants were identified by PCR as described (Soriano *et al*., 1991). The following primers were used to detect a 3.5-kb band indicative of homologous recombination at the *I-mf* locus: a third intron primer lying just upstream of the *Pst*I site at the 5′ end of the targeting vector (5′-AATCAATGTGCCTCCTAGATCTCTCTAGCC-3′) and a sense strand oligonucleotide from the 3′ end of the *neo* gene (Primer 3; 5′-TCGCAGCGCATCGCCTTCTA-3′). Samples were amplified for 40 cycles (93°C for 30 s; 57°C for 30 s; 65°C for 4 min). A total of 165 G418- and gancyclovir-resistant clones were picked and expanded; 16 of them displayed recombination at the *I-mf* (*Mdfi*) locus. Thus, the targeting frequency with the double selection is 10%. Confirmation of *I-mfa* targeting was carried out by Southern blotting with random hexamer [^{32}P]dCTP-labeled DNA probes (Feinberg and Vogelstein, 1983). The 5′-flanking probe was generated by PCR amplification of *I-mfa* Exon III which lies 5′ of the targeting vector, using the following primers: 5′-ACGGATCCCCAGACCATGTCCCTCCTC-3′ (sense) and 5′-CTGGATCCTCACAGC TTCTGTGGGGACATCGAG-3′ (antisense). A 3′-flanking probe and a *neo* probe confirmed the expected recombination events (not shown).

Four of the correctly targeted ES cell lines (lines 91, 133, 184 and 214) were used to generate chimeras by injection of ES cells into 3.5-day C57Bl/6 blastocysts that were transferred to CD1 pseudopregnant foster mothers. Chimeric males were mated with C57Bl/6 females (Jackson Laboratory) and germline transmission of the mutant allele was verified by Southern blot (as above) and PCR analysis (see below) from F_1 offspring with agouti coat color. Two injected ES colonies contributed to the germline of mice. F_2 offspring from heterozygous intercrosses were again genotyped by Southern blotting and PCR.

PCR analysis of I-mfa genotypes

PCR genotyping was performed on genomic DNA of embryonic yolk sacs or tail biopsies of 7-day-old pups. Visceral yolk sacs or tail biopsies were lysed in 100 mM NaCl, 10 mM Tris–HCl pH 8.0, 25 mM EDTA, 0.5% SDS, 100 μg/ml proteinase K and digested overnight at 56°C. DNA was prepared by phenol:chloroform extractions and ethanol precipitation, and resuspended in 500 μl TE buffer (10 mM Tris–HCl pH 8.0, 0.1 mM EDTA). Five microliters of the samples was subjected to PCR analysis using primers 1 (5′-GCCCACCGGAAGTTGCAGACG-3′; sense primer; from *I-mf* Intron III) and Primer 2 (5′-CTTTGATGATGGGCTGTGATCTG-3′; antisense primer; from *I-mf* Exon IV) to detect the wild-type allele (amplification of a 528-bp fragment), while Primer 1 and the *neo* primer (Primer 3, see above) were used to detect the recombinant allele (amplification of a 776-bp fragment). Temperature cycling conditions were: 94°C for 30 s, 57°C for 30 s, and 65°C for 2 min.

RNA isolation and analysis

Total RNA was isolated according to the single-step procedure described by Chomczynski and Sacchi (1987). Quantitative RT–PCR was carried out as described (Rupp and Weintraub, 1991). An initial titration was carried out to assure that amplifications at high cycle numbers were still in the linear range and quantitative. All primer sets were designed to span at least one intron to distinguish RNA from DNA contamination. Subsequent to reverse transcription of RNA (Rupp and Weintraub, 1991), one-fifth of the generated cDNA was added to a 25 μl PCR reaction, using conditions described by Soriano *et al*. (1991). Cycling conditions were as follows: denaturation at 93°C for 30 s, primer annealing at 57°C for 30 s, and primer extension at 65°C for 1 min. The *EF-1*α control was amplified with primers consisting of 5′-AGTTTGAGAAGGAGGCTGCT-3′ (sense) and 5′-CAACAATCAGGACAGCACAGTC-3′ (antisense; 22 cycles; primers generate a 228-bp fragment). *I-mfa* was amplified with primers consisting of 5′-CAGAATTCACAGCCTCAAGGGAACCCC-3′ (sense) and 5′-AACTTGTCTGGTGTCAAAAATAATAGTCTAGAGCG-3′ (antisense; 28 cycles; 240-bp fragment); *I-mfb* was amplified with primers 5′-ACGGATCCCCAGACCATGTCCCTCCTC-3′ (sense) and 5′-ATGGATCCGAACTCTTTTCCCACCCCGTG-3′ (antisense; 30 cycles; 672-bp fragment); *I-mfc* was amplified with primers 5′-AGCGCGCAGCTTGCACGAGTA-3′ (sense) and 5′-TAGCTCGAGCTAACTGGTTCTGTCCTA-3′ (antisense; 30 cycles; 620-bp fragment); and *Scleraxis* was amplified with primers 5′-ATGGATCCCAGCGCCGCCGCCGGGTCGCTA-3′ (sense) and 5′-ATGGATCCCTAACTTCGAATCGCCGTCTT-3′ (antisense; 28 cycles; full-length cDNA). Northern blot analysis was carried out as described previously (Kraut *et al*., 1994), using probes from the same fragments used for the *in situ* hybridization procedure (see below), with the exception of Figure 1D, where an *I-mf* probe used was derived from nucleotides 1–379 of pCS-I-mfa (Chen *et al*., 1996) generated by digesting with *Eco*RI and *Sph*I (this probe detects all three isoforms).

Histological and skeletal analysis

The day the vaginal plug was observed was considered as embryonic day 0.5 (E0.5). Embryos were fixed in 4% paraformaldehyde, embedded in paraffin, sectioned at 5 μm and stained with hematoxylin and eosin. Cartilages and bones were stained with alcian blue and alizarin red by the following method. After removing skin and viscera, embryos were dehydrated in 95% ethanol for 24 h and acetone for 1–3 days, stained in 0.015% alcian blue, 0.005% alizarin red, 5% acetic acid in 70% ethanol for 4–6 h at 37°C and overnight at room temperature, cleared in 96% ethanol for 1 h and 0.5–1% KOH for 24–48 h and further cleared by transfer to solutions of decreasing KOH strength and increasing glycerol concentration.

In situ hybridization

In situ hybridizations using ^{35}S-labeled cRNA were performed as described previously (Hurlin *et al*., 1995; Chen *et al*., 1996). The following murine cDNAs were used in this study as templates for synthesizing antisense riboprobes in the presence of both [^{35}S]CTP and [^{35}S]UTP: *I-mfa* (Chen *et al*., 1996), *Myf5* (Chen *et al*., 1996), *Scleraxis* (Cserjesi *et al*., 1995a), *Pax-1* (Deutsch *et al*., 1988), *Pax-3* (Goulding *et al*., 1991), *Pax-9* (Neubüser *et al*., 1995), *PL-I* (Guillemot *et al*., 1994), *4311* (Lescisin *et al*., 1988), *Mash2* (Guillemot *et al*., 1994), *Hand1* and *Hand2* (Cserjesi *et al*., 1995b), *Mox-1* (Candia *et al*., 1992) and *Paraxis* (Burgess *et al*., 1996). Slides were examined under dark-field and epifluorescence illumination with a Zeiss axioplan microscope.

TUNEL and proliferation assays

The TUNEL reaction to detect incorporation of biotinylated dUTP mediated by terminal transferase was carried out on sectioned embryos as described (Gavrieli *et al*., 1992) except that slides were microwaved for 2 min in 10 mM sodium citrate pH 6.0. Vectastain ABC reagent (Vector Laboratories) was used according to the manufacturer's instructions, and development was carried out with DAB substrate (Vector). A DNase I-treated section was included in each experiment as a positive control. Sections were then counterstained with Gill's hematoxylin #3. Proliferating cells were detected in sections of embryos labeled for 1 h by injection of pregnant females with 100 μg BrdU/g bodyweight, using a monoclonal antibody to BrdU (Boehringer Mannheim) and detection with Vectastain ABC reagent and DAB (Vector).

Cell transfection and CAT assays

The protein coding regions of mouse *Mash2*, *myogenin* and *E12* were PCR-amplified and subcloned into the *Eco*RI–*Xho*I sites of the mammalian expression vector pCS2 (Turner and Weintraub, 1994). pCS2I-mfa has been described previously (Chen *et al*., 1996) and pCS2Hand1 was obtained from S.Hollenberg (Vollum Institute, Portland, OR). NIH 3T3 cells were grown and transfected with bHLH expression

constructs and increasing amounts of CS2I-mfa and the CAT activity of a p4R–CAT reporter construct was determined as described (Chen *et al*., 1996). Rcho-1 cells were maintained in NCTC-135 medium (Sigma) as described previously (Faria and Soares, 1991; Cross *et al*., 1995). Cells were transfected using Superfect reagent (Qiagen). Transient transfections performed to measure promoter activities were performed as described in the figure legends. Mouse placental lactogen-I promoter–CAT constructs (Shida *et al*., 1993) were obtained from D.Linzer (Northwestern University). Stable Rcho-1 transfectants were produced by co-transfecting CS2I-mfa together with a PGK-neo construct (obtained from P.Soriano, FHCRC) and selected for 10 days in 250 μg/ml G418. Transfected cells were pooled and analyzed for I-mfa expression, morphology, cell adhesion and marker expression.

Yeast two-hybrid assay

The protein-coding regions of mouse *myogenin, E12, Mash2, Hand1* and *Id1* were PCR-amplified and subcloned into the *Bam*HI site of pVP16 (Hollenberg *et al*., 1995). Quantitative β-galactosidase activity assays were performed as described (Chen *et al*., 1996).

Acknowledgements

This work is dedicated to the memory of Hal Weintraub. We are grateful to N.Lipnick for her help with genotyping and sectioning of embryos; Dr Y.Zhuang for help with blastocyst injections; Dr P.Soriano for helpful advice and encouragement; Drs M.Bender, R.Eisenman, S.Fiering, S.Hollenberg, S.Parkhurst and C.Queva for valuable discussions; Drs S.Parkhurst, C.Queva, P.Soriano and H.Thirlwell for critical reading of the manuscript; and T.Knight for help with the illustrations. We thank the following colleagues for providing clones for *in situ* hybridizations: Drs J.Rossant and V.Prideaux for PL-1, Mash-2, 4311 and Flt-1; Dr E.Olson for Scleraxis, Paraxis, Hand1 and Hand2; Dr R.Balling for Pax-1 and Pax-9, Dr P.Gruss for Pax-3 and C.Wright for Mox-1. We also thank Drs S.Hollenberg, D.Linzer and E.Olson for reporter constructs, and Dr M.Soares for the Rcho-1 cell line. This work was supported by a fellowship from the Human Frontier Science Program to N.K., NIH grant CA54337 to M.G., and NIH grant AR45113.

References

Bain,G. *et al*. (1994) E2A proteins are required for proper B cell development and initiation of immunoglobulin gene rearrangements. *Cell*, **79**, 885–892.

Braun,T., Rudnicki,M.A., Arnold,H.-H. and Jaenisch,R. (1992) Targeted inactivation of the muscle regulatory gene *myf-5* results in abnormal rib development and perinatal death. *Cell*, **71**, 369–382.

Burgess,R., Rawls,A., Brown,D., Bradley,A. and Olson,E.N. (1996) Requirement of the *paraxis* gene for somite formation and musculoskeletal patterning. *Nature*, **384**, 570–573.

Candia,A.F., Hu,J., Crosby,J., Lalley,P.A., Noden,D., Nadeau,J.H. and Wright,C.V.E. (1992) *Mox-1* and *Mox-2* define a novel homeobox gene subfamily and are differentially expressed during early mesodermal patterning in mouse embryos. *Development*, **116**, 1123–1136.

Carney,E.W., Prideaux,V., Lye,S.J. and Rossant,J. (1993) Progressive expression of trophoblast-specific genes during formation of mouse trophoblast giant cells *in vitro*. *Mol. Reprod. Dev.*, **34**, 357–368.

Chen,C.-M.A., Kraut,N., Groudine,M. and Weintraub,H. (1996) I-mf, a novel myogenic repressor, interacts with members of the MyoD family. *Cell*, **86**, 731–741.

Chomczynski,P. and Sacchi,N. (1987) Single-step method of RNA isolation by acid guanidinium thiocyanate–phenol–chloroform extraction. *Anal. Biochem.*, **162**, 156–159.

Copp,A.J. (1994) Genetic models of mammalian neural tube defects. In *Neural Tube Defects*. Ciba Foundation Symposium No. 181. Wiley, Chichester, pp. 118–143.

Copp,A.J. (1995) Death before birth: clues from gene knockouts and mutations. *Trends Genet.*, **11**, 87–93.

Cross,J.C., Werb,Z. and Fisher,S.J. (1994) Implantation and the placenta: key pieces of the development puzzle. *Science*, **266**, 1508–1518.

Cross,J.C., Flannery,M.L., Blanar,M.A., Steingrimsson,E., Jenkins,N.A., Copeland,N.G., Rutter,W.J. and Werb,Z. (1995) *Hxt* encodes a basic helix–loop–helix transcription factor that regulates trophoblast cell development. *Development*, **121**, 2513–2523.

Cserjesi,P., Brown,D., Ligon,K.L., Lyons,G.E., Copeland,N.G., Gilbert,D.J., Jenkins,N.A. and Olson,E.N. (1995a) Scleraxis: a basic helix–loop–helix protein that prefigures skeletal formation during mouse embryogenesis. *Development*, **121**, 1099–1110.

Cserjesi,P., Brown,D., Lyons,G.E. and Olson,E.N. (1995b) Expression of the novel basic helix–loop–helix gene *eHAND* in neural crest derivatives and extraembryonic membranes during mouse development. *Dev. Biol.*, **170**, 664–678.

Deutsch,U., Dressler,G.R. and Gruss,P. (1988) *Pax1*, a member of a paired box homologous murine gene family, is expressed in segmented structures during development. *Cell*, **53**, 617–625.

Ellmeier,W. and Weith,A. (1995) Expression of the helix–loop–helix gene *Id3* during murine embryonic development. *Dev. Dyn.*, **203**, 163–173.

Faria,T.N. and Soares,M.J. (1991) Trophoblast cell differentiation: establishment, characterization, and modulation of a rat trophoblast cell line expressing members of the placental prolactin family. *Endocrinology*, **129**, 2895–2906.

Feinberg,A.J. and Vogelstein,B. (1983) A technique for radiolabelling DNA restriction endonuclease fragments to high specific activity. *Anal. Biochem.*, **132**, 6–13.

Firulli,A.B., McFadden,D.G., Lin,Q., Srivastava,D. and Olson,E.N. (1998) Heart and extra-embryonic mesodermal defects in mouse embryos lacking the bHLH transcription factor Hand1. *Nature Genet.*, **18**, 266–270.

Gavrieli,Y., Sherman,Y. and Ben-Sasson,S.A. (1992) Identification of programmed cell death *in situ* via specific labeling of nuclear DNA fragmentation. *J. Cell Biol.*, **119**, 493–501.

Goulding,M.D., Chalepakis,G., Deutsch,U., Erselius,J. and Gruss,P. (1991) Pax-3, a novel murine DNA binding protein expressed during early neurogenesis. *EMBO J.*, **10**, 1135–1147.

Guillemot,F., Nagy,A., Auerbach,A., Rossant,J. and Joyner,A.L. (1994) Essential role of *Mash-2* in extraembryonic development. *Nature*, **371**, 333–336.

Hogan,B., Beddington,R., Costantini,F., and Lacy,E. (1994) *Manipulating the Mouse Embryo: A Laboratory Manual.* Cold Spring Harbor Laboratory Press, Cold Spring Harbor, NY.

Hollenberg,S.M., Sternglanz,R., Cheng,P.F. and Weintraub,H. (1995) Identification of a new family of tissue-specific basic helix–loop–helix proteins with a two-hybrid system. *Mol. Cell. Biol.*, **15**, 3813–3822.

Hurlin,P.J., Quéva,C., Koskinen,P.J., Steingrímssan,E., Ayer,D.E., Copeland,N.G., Jenkins,N.A. and Eisenman,R.N. (1995) Mad3 and Mad4: novel Max-interacting transcriptional repressors that suppress c-*myc* dependent transformation and are expressed during neural and epidermal differentiation. *EMBO J.*, **14**, 5646–5659.

Ilgren,E.B. (1983) Control of trophoblastic growth. *Placenta*, **4**, 307–328.

Jan,Y.N. and Jan,L.Y. (1993) HLH proteins, fly neurogenesis, and vertebrate myogenesis. *Cell*, **75**, 827–830.

Jen,Y., Weintraub,H. and Benezra,R. (1992) Overexpression of Id protein inhibits the muscle differentiation program: *in vivo* association of Id with E2A proteins. *Genes Dev.*, **6**, 1466–1479.

Kraut,N. (1997) The gene encoding I-mf (*Mdfi*) maps to human Chromosome 6p21 and mouse Chromosome 17. *Mamm. Genome*, **8**, 618–619.

Kraut,N., Frampton,J., McNagny,K.M. and Graf,T. (1994) A functional Ets DNA-binding domain is required to maintain multipotency of hematopoietic progenitors transformed by Myb-Ets. *Genes Dev.*, **8**, 33–44.

Lee,J.E. (1997) Basic helix–loop–helix genes in neural development. *Curr. Opin. Neurobiol.*, **7**, 13–20.

Lescisin,K.R., Varmuza,S. and Rossant,J. (1988) Isolation and characterization of a novel trophoblast-specific cDNA in the mouse. *Genes Dev.*, **2**, 1639–1646.

Liu,Y., Watanabe,H., Nifuji,A., Yamada,Y., Olson,E.N. and Noda,M. (1997) Overexpression of a single helix–loop–helix-type transcription factor, scleraxis, enhances aggrecan gene expression in osteoblastic osteosarcoma ROS17/2.8 cells. *J. Biol. Chem.*, **272**, 29880–29885.

Morriss-Kay,G., Wood,H. and Chen,W.H. (1994) Normal neurulation in mammals. *In Neural Tube Defects*. Ciba Foundation Symposium No. 181, Wiley. Chichester, pp. 51–63.

Nagy,A., Gocza,E., Merentes Diaz,E., Prideaux,V.R., Ivanyi,E., Markkula,M. and Rossant,J. (1990) Embryonic stem cells alone are able to support fetal development in the mouse. *Development*, **110**, 815–821.

Neubüser,A., Koseki,H. and Balling,R. (1995) Characterization and developmental expression of *Pax9*, a paired-box-containing gene related to *Pax1*. *Dev. Biol.*, **170**, 701–716.

Riley,P., Anson-Cartwright,L. and Cross,J.C. (1998) The Hand1 bHLH transcription factor is essential for placentation and cardiac morphogenesis. *Nature Genet.*, **18**, 271–275.

Rudnicki,M.A. and Jaenisch,R. (1995) The MyoD family of transcription factors and skeletal myogenesis. *BioEssays*, **17**, 203–209.

Rugh,R. (1990) *The Mouse, its Reproduction and Development.* Oxford University Press, New York.

Rupp,R.A.W. and Weintraub,H. (1991) Ubiquitous MyoD transcription at the midblastula transition precedes induction-dependent expression in the presumptive mesoderm. *Cell*, **65**, 927–937.

Sasai,Y., Kageyama,R., Tagawa,Y., Shigemoto,R. and Nakanishi,S. (1992) Two mammalian helix–loop–helix factors structurally related to *Drosophila* hairy and Enhancer of split. *Genes Dev.*, **6**, 2620–2634.

Shida,M.M., Ng,Y.K., Soares,M.J. and Linzer,D.I.H. (1993) Trophoblast-specific transcription from the mouse placental lactogen-I gene promoter. *Mol. Endocrinol.*, **7**, 181–188.

Shivdasani,R.A., Mayer,E.L. and Orkin,S.H. (1995) Absence of blood formation in mice lacking the T-cell leukaemia oncoprotein tal-1/SCL. *Nature*, **373**, 432–434.

Sibilia,M. and Wagner,E.F. (1995) Strain-dependent epithelial defects in mice lacking the EGF receptor. *Science*, **269**, 234–238.

Soriano,P., Montgomery,C., Geske,R. and Bradley,A. (1991) Targeted disruption of the c-*src* proto-oncogene leads to osteopetrosis in mice. *Cell*, **64**, 693–702.

Spicer,D.B., Rhee,J., Cheung,W.L. and Lassar,A.B. (1996) Inhibition of myogenic bHLH and MEF2 transcription factors by the bHLH protein twist. *Science*, **272**, 1476–1480.

Srivastava,D., Thomas,T., Lin,Q., Kirby,M.L., Brown,D. and Olson,E.N. (1997) Regulation of cardiac mesodermal and neural crest development by the bHLH transcription factor, dHAND. *Nature Genet.*, **16**, 154–160.

Tanaka,M., Gertsenstein,M., Rossant,J. and Nagy,A. (1997) Mash2 acts cell autonomously in mouse spongiotrophoblast development. *Dev. Biol.*, **190**, 55–65.

Threadgill,D.W. *et al*. (1995) Targeted disruption of mouse EGF receptor: effect of genetic background on mutant phenotype. *Science*, **269**, 230–234.

Turner,D. and Weintraub,H. (1994) Expression of achaete scute homologue 3 in *Xenopus* embryos converts ectodermal cells to a neural fate. *Genes Dev.*, **8**, 1434–1447.

Tybulewicz,V.L.J., Crawford,C.E., Jackson,P.K., Bronson,R.T. and Mulligan,R.C. (1991) Neonatal lethality and lymphopenia in mice with a homozygous disruption of the c-*abl* proto-oncogene. *Cell*, **65**, 1153–1163.

Wallin,J., Wilting,J., Koseki,H., Fritsch,R., Christ,B. and Balling,R. (1994) The role of *Pax-1* in axial skeleton development. *Development*, **120**, 1109–1121.

Wang,Y., Benezra,R. and Sassoon,D.A. (1992) *Id* expression during mouse development: a role in morphogenesis. *Dev. Dyn.*, **194**, 222–230.

Weintraub,H. (1993) The MyoD family and myogenesis: redundancy, networks, and thresholds. *Cell*, **75**, 1241–1244.

Weintraub,H. *et al*. (1991) The *myoD* gene family: nodal point during specification of muscle cell lineage. *Science*, **251**, 761–766.

Wolf,C., Thisse,C., Stoetzel,C., Thisse,B., Gerlinger,P. and Perrin-Schmitt,F. (1991) The *M-twist* gene of *Mus* is expressed in subsets of mesodermal cells and is closely related to the *Xenopus X-twi* and the *Drosophila twist* gene. *Dev. Biol.*, **143**, 363–373.

Yoon,J.K., Olson,E.N., Arnold,H.-H. and Wold,B.J. (1997) Different MRF4 knockout alleles differentially disrupt *Myf-5* expression: cis-regulatory interactions at the *MRF4/Myf-5* locus. *Dev. Biol.*, **188**, 349–362.

Zhuang,Y., Soriano,P. and Weintraub,H. (1994) The helix–loop–helix gene *E2A* is required for B cell formation. *Cell*, **79**, 875–884.

Received July 16, 1998; revised September 2, 1998; accepted September 3, 1998